JGR Oceans

RESEARCH ARTICLE
10.1029/2018JC014805

Special Section:
Forum for Arctic Modeling and Observational Synthesis (FAMOS) 2: Beaufort Gyre phenomenon

Variations in Rates of Biological Production in the Beaufort Gyre as the Arctic Changes: Rates From 2011 to 2016

Brenda Y. Ji[1], Zoe O. Sandwith[2], William J. Williams[3], Oana Diaconescu[1], Rubao Ji[2], Yun Li[4], Emma Van Scoy[1], Michiyo Yamamoto-Kawai[5], Sarah Zimmermann[3], and Rachel H. R. Stanley[1]

[1]Department of Chemistry, Wellesley College, Wellesley, MA, USA, [2]Woods Hole Oceanographic Institution, Woods Hole, MA, USA, [3]Fisheries and Oceans Canada, Institute of Ocean Sciences, Sidney, British Columbia, Canada, [4]College of Marine Science, University of South Florida, St. Petersburg, FL, USA, [5]Department of Marine Ocean Sciences, Tokyo University of Marine Science and Technology, Minato-ku, Japan

Abstract The Arctic Ocean is experiencing profound environmental changes as the climate warms. Understanding how these changes will affect Arctic biological productivity is key for predicting future Arctic ecosystems and the global CO_2 balance. Here we use in situ gas measurements to quantify rates of gross oxygen production (GOP, total photosynthesis) and net community production (NCP, net CO_2 drawdown by the biological pump) in the mixed layer in summer or fall from 2011 to 2016 in the Beaufort Gyre. NCP and GOP show spatial and temporal variations with higher values linked with lower concentrations of sea ice and increased upper ocean stratification. Mean rates of GOP range from 8 ± 1 to 54 ± 9 mmol $O_2 \cdot m^{-2} \cdot d^{-1}$ with the highest mean rates occurring in summer of 2012. Mean rates of NCP ranged from 1.3 ± 0.2 to 2.9 ± 0.5 mmol $O_2 \cdot m^{-2} \cdot d^{-1}$. The mean ratio of NCP/GOP, a measure of how efficiently the ecosystem is recycling its nutrients, ranged from 0.04 to 0.17, similar to ratios observed at lower latitudes. Additionally, a large increase in total photosynthesis that occurred in 2012, a year of historically low sea ice coverage, persisted for many years. Taken together, these data provide one of the most complete characterizations of interannual variations of biological productivity in this climatically important region, can serve as a baseline for future changes in rates of production, and give an intriguing glimpse of how this region of the Arctic may respond to future lack of sea ice.

Plain Language Summary The Arctic Ocean is changing rapidly because of global climate change. Sea ice is declining, with the Arctic expected to be ice-free in the summer by the middle of this century. The effect of these environmental changes on the marine carbon cycle is poorly known. In this study, rates of marine photosynthesis and net carbon dioxide drawdown in the summer or fall of 2011–2016 show that ice concentration was the largest environmental predictor of biological productivity, with smaller sea ice concentrations leading to increased rates of photosynthesis and thus likely to higher carbon dioxide drawdown. Additionally, a large increase in total photosynthesis that occurred in 2012, a year of historically low sea ice coverage, persisted for many years. An alternative hypothesis for the large increase in photosynthesis in 2012 is that the data in 2011 were collected before the onset of summer stratification (time when mixed layer depth gets very shallow), whereas data for all subsequent years were collected after this increase in stratification had occurred.

Key Points:
- Sea ice concentration is the environmental factor that has the strongest correlation with net community production and photosynthesis
- Rates of net community production and total photosynthesis were significantly positively correlated with N^2, an index of stratification
- One interpretation suggests that as sea ice melts, the gyre will have large increases in photosynthesis but small ones in net CO_2 drawdown

Supporting Information:
- Supporting Information S1

Correspondence to: R. H. R. Stanley,
rachel.stanley@wellesley.edu

Citation:
Ji, B. Y., Sandwith, Z. O., Williams, W. J., Diaconescu, O., Ji, R., Li, Y., et al. (2019). Variations in rates of biological production in the Beaufort Gyre as the Arctic changes: Rates from 2011 to 2016. Journal of Geophysical Research: Oceans, 124. https://doi.org/10.1029/2018JC014805

Received 23 NOV 2018
Accepted 23 APR 2019
Accepted article online 30 APR 2019

1. Introduction

Profound environmental changes are occurring in the Arctic, one of the regions experiencing the effects of global warming most severely. Sea ice is melting, with sea ice in recent years consistently being 2 standard deviations below the previous 30-year mean. In particular, all 10 lowest Arctic September sea ice extents compared to the past several decades were measured in the last 10 years (Petty et al., 2018) and the Arctic is expected to be ice-free in summertime by the middle of this century (Jahn et al., 2016). Additionally, terrigenous input is increasing (Abbott et al., 2016), the seawater is freshening (Carmack et al., 2016), and temperatures are warming (Boisvert & Stroeve, 2015). Stratification is expected to increase (Nummelin et al., 2016), which should lead to increased light regimes but lower levels of nutrients.

The Arctic Ocean is currently a disproportionately large carbon sink for its area (Bates et al., 2011) but the fate of the Arctic Ocean as a carbon sink as the environment changes is highly uncertain, in part because the response of autotrophic and heterotrophic communities to the changes is not well known. Due to the recent and drastic declines in sea ice extent in the Arctic Ocean, studies have suggested that the once light-limited environment could host larger phytoplankton blooms that could lead to more primary production and therefore a greater uptake of carbon (Slagstad et al., 2015). Moreover, an additional fall phytoplankton bloom in the Arctic Ocean, where there is normally only an annual spring bloom, could have profound implications on biological productivity and the carbon cycle (Ardyna et al., 2014). These changes in the timing of blooms are also suspected to alter the zooplankton community and their grazing pressures on phytoplankton (Ji et al., 2013).

However, nutrients also play an important role in phytoplankton growth and primary productivity (Tremblay et al., 2015) and an increasingly stratified upper ocean and a growing microbial community due to increased light penetration could deplete the nutrient supply in the Arctic Ocean (McLaughlin & Carmack, 2010) and thus lead to less CO_2 drawdown (Cai et al., 2010). Additionally, the existence of phytoplankton blooms under the sea ice (Arrigo et al., 2012) suggest that an ice-free Arctic Ocean could possibly lead to a decrease in overall productivity as the under-ice habitats would be diminished if the sea ice disappears too early in the season. In short, the uncertainty in the fate of the Arctic Ocean as a carbon sink calls for accurate measurements of biological productivity over different years and times in order to improve understanding on how environmental factors are affecting rates of biological productivity currently.

Gross primary production refers to the total rate of photosynthesis. When measured by tracking changes in oxygen, a product of photosynthesis, the rate is called gross oxygen production (GOP) to account for the fact that some production of oxygen could be due to the Mehler reaction or other noncarbon fixing processes (Juranek & Quay, 2013). Net community production (NCP) equals the rate of photosynthesis minus autotrophic and heterotrophic respiration and thus is a measure of the net amount of CO_2 drawn down by the biological pump as modulated by the Revelle factor. On long enough spatial and temporal scales, net community production equals export production (Estapa et al., 2015). In this study, we used the gas tracer triple oxygen isotopes and O_2/Ar to measure in situ rates of GOP and NCP at more than 30 locations in the Beaufort Gyre region of the Canada Basin each year, over a period of six years. The Canada Basin is one of the Arctic's most oligotrophic regions (Varela et al., 2013).

GOP and NCP calculated from the gas tracers provide an exponentially weighted average of production over approximately the previous 6 to 20 days (Teeter et al., 2018). The rates are only for the mixed layer and thus will not include any production occurring in the region between the bottom of the mixed layer and the bottom of the euphotic zone. The Arctic has large subsurface chlorophyll maxima, and this method unfortunately will not quantify production associated with the subsurface chlorophyll maxima. Thus, the rates presented in this paper are a lower bound for total NCP and GOP. A nitrate uptake study has shown that although having high chlorophyll, the subsurface chlorophyll maximum is responsible for very little production in the Canada Basin (Ardyna et al., 2013; Varela et al., 2013). Additionally, the rates of primary production in the Beaufort Sea/Canada Basin were generally uniform with depth (Varela et al., 2013), suggesting that even if the total rates of production reported here underestimate the total integrated production, as is likely, they probably do so by similar amount across the stations. Thus, the patterns (spatial and temporal) and the connections to environmental variables (such as ice cover) are likely similar whether total GOP and NCP is considered or whether only mixed layer GOP and NCP are examined.

Data from three approximately monthlong summer cruises (2011, 2012, and 2013) as well as three approximately monthlong fall cruises (2014, 2015, 2016) allow a glimpse of interannual and seasonal variability in productivity and also the response of the carbon cycle in this region of the Arctic to a variety of environmental conditions. The 2011 cruise was before the onset of summer stratification, whereas the 2012 and 2013 cruises were also in the summer but two weeks later and thus after the summer increase in stratification had occurred. A variety of chemical and physical measurements, such as the nutrients silicate, phosphate and nitrate, temperature, and salinity, were made concurrently with the production rates. The years studied encompass the year of lowest sea ice extent in the Arctic (2012) when the sampling grid was almost ice free as well as years with relatively more total ice (2013 and 2014).

2. Materials and Methods

2.1. Cruise Description

All samples were collected on the CCGS Louis S. St-Laurent as part of the Joint Ocean Ice Study/Beaufort Gyre Observing System cruises. The cruises took place in summer in 2011, 2012, and 2013 and in fall in 2014, 2015, and 2016 between 70 and 81°N and 131°W to 176°W. See Table S1 for a listing of exact dates of each cruise. Exact sample locations are shown in Figure 1.

2.2. Gas Tracers

Seawater was collected from the surface ($z < 6$ m) 12-L Niskin bottle on a 24-bottle CTD rosette at stations on the cruises and directed into preevacuated and prepoisoned with mercuric chloride custom-made 500-mL sampling flasks (Emerson et al., 1999). The bottles were brought to Woods Hole Oceanographic Institution where they were drained of seawater, and the oxygen and argon gas contained in the sample was analyzed on a custom-built triple oxygen isotope processing line attached to a Thermo Fisher 253 isotope ratio mass spectrometer (Barkan & Luz, 2003; Stanley et al., 2015). Reproducibility based on duplicate samples taken throughout the six years of the program of $\delta^{17}O$ was 0.02‰, $\delta^{18}O$ was 0.01‰, Δ^{17} was 5 per meg, and $\delta O_2/Ar$ was 0.8‰. All data are available from the NSF Arctic Data Center. These analytical uncertainties propagate into an approximately 10% uncertainty in the estimates of GOP and 1% uncertainty in the estimate of NCP.

2.3. GOP and NCP Calculations

Rates of mixed layer GOP were calculated from the $\delta^{17}O$ and $\delta^{18}O$ according to the steady state equation (6) of Prokopenko et al. (2011), with photosynthetic end-member determined from the measured $\delta^{18}O\text{-}H_2O$ on samples from the same cruise (Manning et al., 2017), assumption that $^{17}\Delta$ excess of seawater $= 0$ and using other constants as stated in Manning et al. (2017). On the few samples that $\delta^{18}O\text{-}H_2O$ was not available, $\delta^{18}O\text{-}H_2O$ was estimated from a relationship with salinity from all the measured samples from that year. Including the measured $\delta^{18}O\text{-}H_2O$ is important in the Arctic—neglecting it can lead to errors of up to 50% (Manning et al., 2017). Varying the $^{17}\Delta$ excess of seawater by 8 per meg (2 standard deviations of the global average (Luz & Barkan, 2010)) changes the GOP estimate by 5–6% on average (Manning et al., 2017). The combined error in the calculations excluding the contribution from gas transfer velocity is 12% for GOP. NCP was calculated from O_2/Ar from the bottle samples, according to Hendricks et al. (2004). The equations used to calculate NCP and GOP assume steady state and negligible mixing across the base of the mixed layer. Given the very strong stratification in this region, the latter assumption is reasonable. The correction equations described in Nicholson et al. (2014) in combination with vertical profiles collected at a subset of the stations were used to confirm that contributions from vertical entrainment and mixing were less than 1% of the calculated rates of production.

The steady state assumption is more nuanced given that the production in the marginal ice zone especially may not be in steady state. However, recent work has shown that when steady state is assumed, the gas tracer-derived NCP rates are giving a production rate that is exponentially averaged over several residence times of the gas tracer in the system (Teeter et al., 2018). Since ventilation is the main process affecting these gases, the residence time can be estimated by dividing the mixed layer depth by the gas transfer velocity. Therefore, residence times are shorter in the summer when the mixed layers are very shallow. The residence times in the summer were a few days and in the fall were one to two weeks. Thus, the rates presented here represent the production in the Beaufort Gyre exponentially averaged over a time scale of days in the summer cruises and weeks in the fall cruises.

For both NCP and GOP calculations, gas transfer velocities were calculated by multiplying a gas transfer velocity calculated based on a quadratic function of wind speed (Stanley et al., 2009) multiplied by the open water fraction (1 − sea ice concentration; Islam et al., 2016). The total gas transfer velocity was calculated as a weighted average of the sea ice scaled gas transfer velocities going back 60 days from the sample collection date (Reuer et al., 2007). Gas transfer velocities in open water have uncertainties of approximately 15 to 20% (Ho et al., 2011; Stanley et al., 2009; Wanninkhof, 2014). In partially ice-covered waters, gas exchange could be enhanced by up to 40% (Loose et al., 2014; Lovely et al., 2015) but parameterizations that take these processes into account are not well established and there is much debate as to whether the open water fraction (Butterworth & Miller, 2016; Prytherch et al., 2017) or the enhanced turbulence model is correct (Fanning &

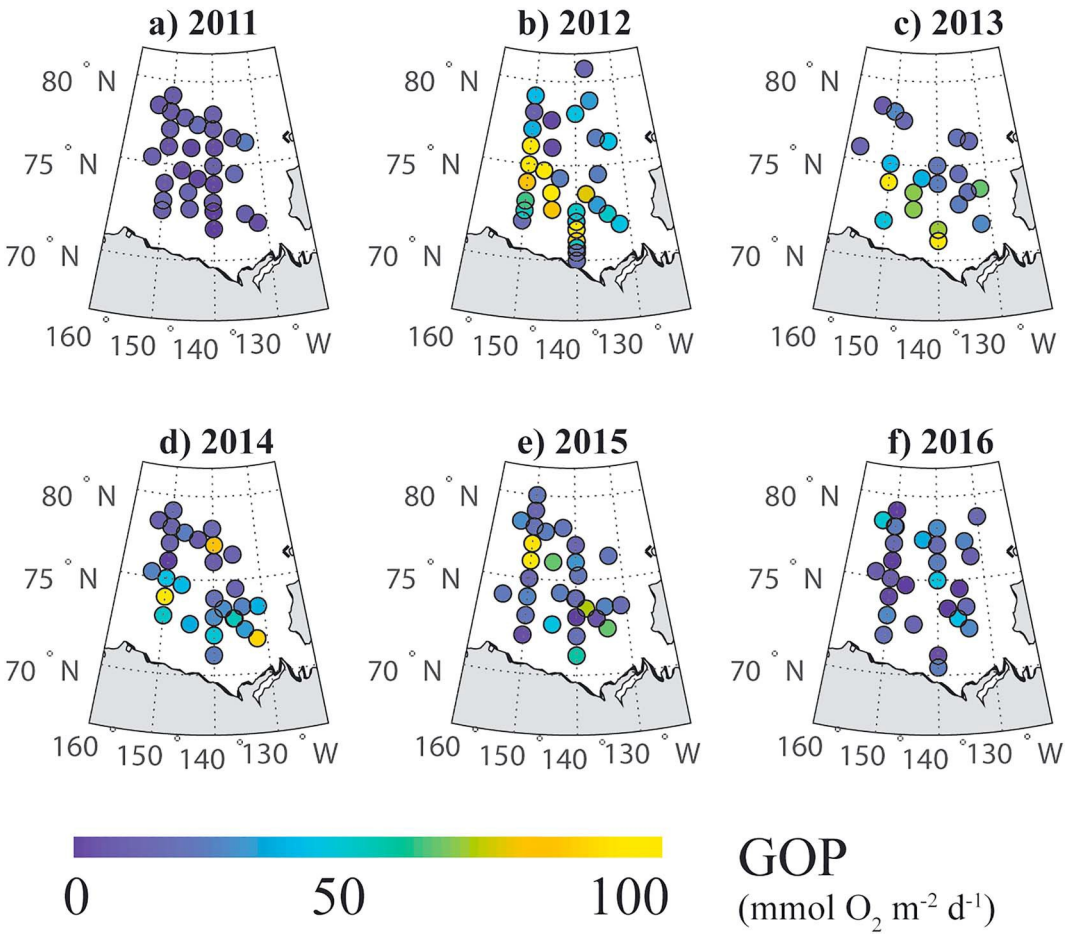

Figure 1. Rates of gross oxygen production (GOP), integrated from the surface to the depth of the mixed layer, in the Beaufort Gyre region of the Canada Basin in the (a–c) summer of 2011, 2012, and 2013 and (d–f) fall of 2014, 2015, and 2016.

Torres, 1991; Loose et al., 2017). Thus, the uncertainty in the gas transfer calculation is by far the largest source of uncertainty in the GOP and NCP estimates.

2.4. Ancillary Data

Sea ice concentration was extracted from the Nimbus-7 SMMR and DMSP SSM/I-SSMIS Passive Microwave Data (Cavalieri et al., 1996) using two functions written by Chad Greene (Greene, 2016) and then interpolated to specific station coordinates.

Stratification index N^2 was calculated from the TEOS-10 Matlab function gsw_Nsquared which is based on the 48 term equation for the buoyancy Brunt-Vaisala frequency squared. Calculations were based on buoyancy gradient between the surface and 50 m for the CTD data. Additionally, in order to look at stratification before the cruise started, N^2 was calculated from profiles obtained by ice-tethered profilers (ITPs) in the region (Krishfield et al., 2008; Toole et al., 2011). The Ice-Tethered Profiler data were collected and made available by the Ice-Tethered Profiler Program based at the Woods Hole Oceanographic Institution (http://www.whoi.edu/itp). For the ITP data, since the profilers' shallowest depth was 10 m, the gradient was calculated between 10- and 50-m depth. When calculations were made for N^2 based on the gradient between the surface and 25 m, the correlations discussed in the above manuscript were very similar.

Nutrients, namely, silicate and phosphate, were analyzed using a three-channel Technicon Auto Analyzer (Barwell-Clarke & Whitney, 1996). The precisions for silicate and phosphate were 0.15 and 0.01 mmol/m^3, respectively. Nitrate was almost always undetectable in the surface measurements of the

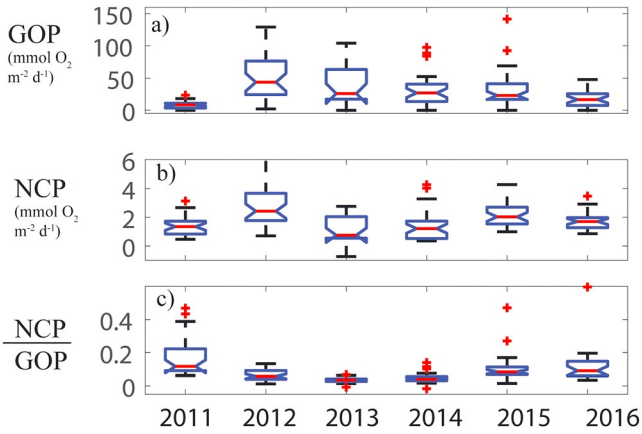

Figure 2. Both spatial and temporal variability in rates is revealed by notched box and whisker plots of (a) GOP, (b) NCP, and (c) NCP/GOP for each of the study years. Medians are red lines, outliers are asterisks, and the box encompasses 25 to 75% of the data. If the notches do not overlap, then there is 95% confidence that the true medians differ.

cruises (detection limit = 0.05 mmol/m^3) and thus is not discussed in this paper. Fluorescence was measured using the Seapoint Chlorophyll Fluorometer, which had a minimum detection level of 0.02 mg/m^3. Total fraction chlorophyll a samples were measured by filtering water samples from Niskin bottles through 0.7-μm GF/F Millipore filters and stored at −80 °C. The precision was 0.01 mg/m^3. The chlorophyll a data were used to calibrate fluorescence data for an algorithm on community composition analysis, which requires chlorophyll fluorescence profile data. Mixed layer depths were calculated from CTD density profiles, using the criterion of a difference in density from the surface of 0.1 kg/m^3. In addition, mixed layer depths were also calculated based on oxygen concentrations (Castro-Morales & Kaiser, 2012) and the resulting values of NCP and GOP were compared to rates calculated with density-based mixed layers. A plot of GOP calculated with a density-based mixed layer depth compared to GOP calculated with an oxygen-based mixed layer depth showed that all but 2 points were within errors of a 1:1 line and that a linear regression fit to the data had a slope = 1.003 ± 0.008. For NCP, a similar plot had all but 4 data points lying on the 1:1 line and the slope was 1.01 ± 0.002. Thus, the productivity results were very similar no matter which technique was used to calculate the mixed layer depth.

3. Results

3.1. Gross Oxygen Production

At most locations, GOP in the Beaufort Gyre region of the Canada Basin is low, with the mean values (within a cruise) being slightly lower than GOP in the subtropical gyres (Juranek & Quay, 2005, 2013; Luz & Barkan, 2009) and much lower than GOP in the Southern Ocean (Reuer et al., 2007), where it has been measured using the same triple oxygen isotope technique. However, mixed layer GOP varied substantially throughout the region each season, suggesting large spatial variability (Figure 1) within our sampling grid. In some years (2012, 2013, 2014), larger values clustered in certain locations within the sampling grid, whereas in other years, there was no apparent pattern to the spatial variability. In particular, within a cruise, rates varied from near 0 to over 60 mmol $O_2 \cdot m^2 \cdot d^{-1}$ (the maximum values depend on the year). Because of the large spatial variability within each sampling season, notched box and whisker plots offer a concise way to viewing both the spatial and the interannual variability in calculated rates of production. Figure 2a shows that mean GOP within the sampling grid for a given cruise increased dramatically (factor of 7) in 2012 compared to 2011 (Table 1). GOP remained much higher than 2011 for the remainder of the time series but gradually decreased each year after 2012 (Figure 2a). In particular, by 2016, mean GOP was only twice the 2011 value. Notably, these rates do not show much seasonal difference with rates from the fall cruises being near equal to the summer cruises (except for 2011). However, the rate of GOP divided by the depth of the mixed layer (calculated using a density criterion of 0.1-kg/m^3 difference from surface) which gives a measure of how much photosynthesis is occurring in a cubic meter of water (hereafter called volumetric GOP), shows a marked difference with summer GOP on a volumetric basis being larger than fall GOP (Figure S1a and Table S2). However, because mixed layers are so much deeper in the fall, the total GOP integrated over the mixed layer is similar in both seasons.

Table 1
Mean Rates of GOP and NCP Integrated Over the Mixed Layer for Each Cruise (in units of mmol $O_2 \cdot m^{-2} \cdot d^{-1}$) and the Mean Ratio of NCP/GOP, a Measure of the Biological Pump Efficiency

Year	GOP	NCP	NCP/GOP
2011	8 (1)	1.4 (0.2)	0.17 (0.03)
2012	54 (9)	2.9 (0.5)	0.11 (0.02)
2013	40 (9)	1.4 (0.3)	0.04 (0.01)
2014	31 (5)	1.3 (0.2)	0.05 (0.01)
2015	32 (5)	2.5 (0.4)	0.11 (0.02)
2016	18 (3)	1.8 (0.3)	0.15 (0.03)

Note. One-sigma standard errors given in parentheses.

3.2. Net Community Production

Mixed layer NCP also varied substantially throughout the region each season (Figure 3), with some years (2011, 2013, and 2014) having higher values in the southern portion of the sampling grid and some years showing no apparent pattern. A notched box and whisker plot (Figure 2b) again show an increase in productivity rate in the very low ice year of 2012. This time, the increase is smaller, however, than in the case of GOP (twofold increase in mean rate). Additionally, rates of NCP in several subsequent

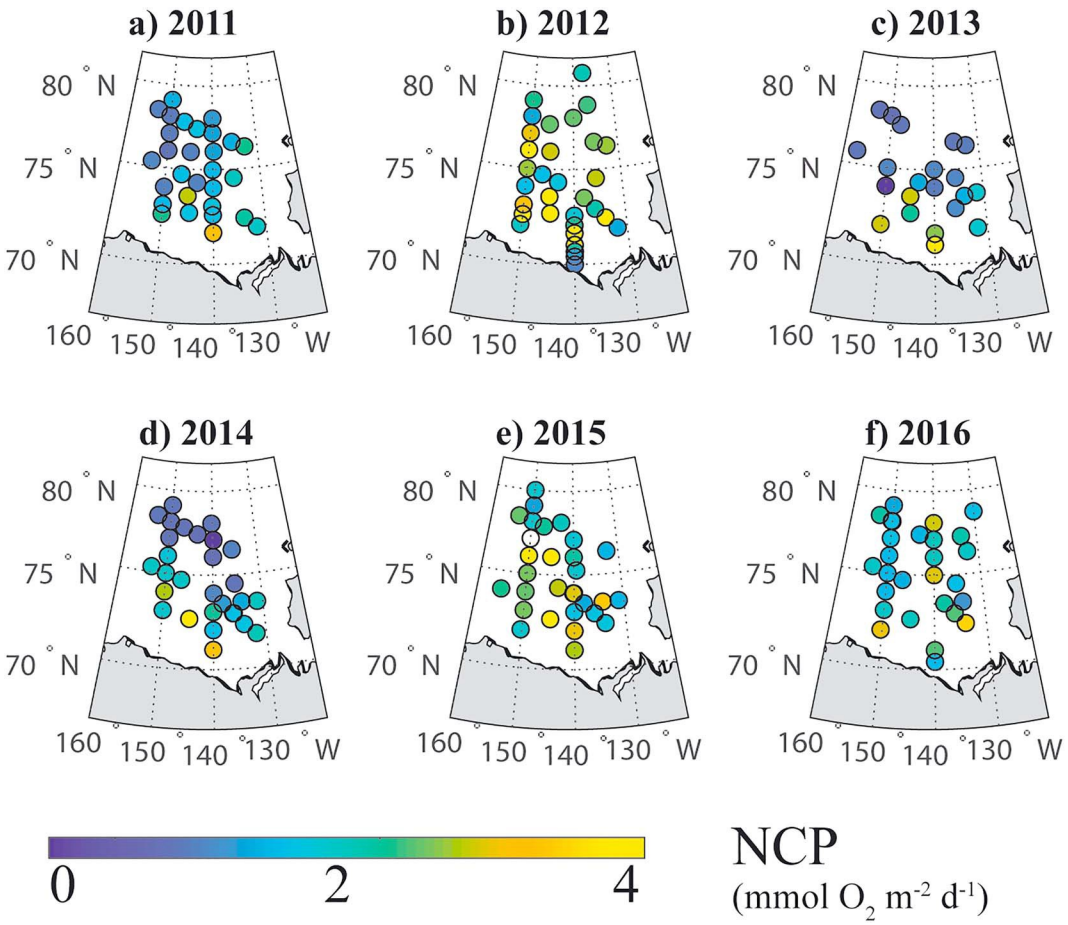

Figure 3. Rates of net community production (NCP), integrated from the surface to the depth of the mixed layer, in the Beaufort Gyre region of the Canada Basin in the (a–c) summer of 2011, 2012, and 2013 and (d–f) fall of 2014, 2015, and 2016.

years (2013, 2014, 2016) are similar to that in 2011, unlike in the case of GOP when a new level seemed to be reached starting in 2012. For NCP, the highest rates occurred in 2012 and 2015. While 2012 had low sea ice extent, 2015 was a year of more typical sea ice cover (Figure S2a). Additionally, 2016 also had low sea ice extent but did not have significantly higher NCP than the years with higher sea ice extent of 2011, 2013, and 2014. Similarly to GOP, the total rate of NCP in the mixed layer is similar in the summer and fall cruises. However, if one considers the volumetric rate, then NCP is larger in the summer than in the fall due to deeper mixed layers in the fall (Figure S1b and Table S2). The NCP rates calculated here from 2012 agree well the mean NCP (4.9 mmol $O_2 \cdot m^{-2} \cdot d^{-1}$) calculated from diel cycles of dissolved oxygen and pCO_2 from ice tethered profilers records in a similar location and timeframe (Islam et al., 2017).

3.3. Biological Pump Efficiency: the NCP/GOP Ratio

The ratio of NCP to GOP is a measure of the efficiency of the biological pump. Higher ratios imply an ecosystem that is inefficient and thus "leaky" with respect to carbon—a larger proportion of the carbon is exported instead of being cycled through the microbial loop. Mean ratios of NCP/GOP vary from 0.05 to 0.17, with some ratios reaching as high as 0.6 depending on the location and year. Year 2011 has the largest and most variable rates of NCP/GOP (Figure 2c). The ratio of NCP/GOP decreased significantly in 2012 compared to 2011. Ratios are lowest in 2013 and 2014, the years with the highest sea ice extent. Notably, nearly all the ratios have values that are similar to what has been observed in lower latitudes (Juranek & Quay, 2013) but lower than what has been observed in some polar field programs (Goldman et al., 2015) and in some Arctic modeling studies (Slagstad et al., 2015).

Table 2
Adjusted R^2 Values from Multilinear Regressions of the Response Variable (GOP, NCP, NCP/GOP) and the Two Predictor Variables of (1) Year (as a Categorical Variable) and (2) the Environmental Variable Listed

Additional Predictor Environmental Variable	Response Variable		
	GOP	NCP	NCP/GOP
Ice concentration	0.30	0.30	0.12
N^2 (stratification)	0.23	0.21	0.10
PO_4	0.23	0.18	0.09
SiO_4	0.24	0.22	-
Mixed layer depth	0.24	0.23	0.07
Day of year	0.23	0.17	0.13
Wind speed	0.20	0.18	0.12
None (only year)	0.22	0.17	0.10

Note. All values listed are significant ($p < 0.05$, $N = 191$). Values in bold are larger than the multilinear regression with the same response variable but only with year as a predictor variable.

3.4. Interannual Variability in Environmental Setting

The ice concentration, stratification index N^2, nutrient levels, mixed layer depth, and wind speeds varied both within a cruise and from year to year. Notched box and whisker plots of these variables are shown in Figure S2 and spatial variability within each year are shown in Figures S4–S7. Ice concentration was lowest in 2012 when virtually the whole sampling grid was completely ice free. The year with next lowest ice concentration was 2016. Highest ice concentrations were observed in 2013 and 2014. The summer cruises (2011, 2012, and 2013) all had higher stratification indices N^2 and deeper mixed layers than the fall cruises (2014, 2015, and 2016). The nutrients phosphate and silicate were similar in most of the years, showing not much seasonal change, with the exception that silicate had significantly lower concentrations in 2011 and that phosphate had significantly higher concentrations in 2013 and 2014. Nitrate was undetectable in the surface waters in all the years. Winds were variable from year to year, showing no definitive seasonal patterns with highest wind speeds being observed in 2012 and 2015.

4. Discussion

4.1. Multilinear Regression Analysis

In order to elucidate connections between environmental variables and rates of productivity, multilinear correlations were calculated between GOP or NCP and an environmental variable (ice cover, stratification index, Brunt Vaisala frequency N^2, phosphate, silicate, mixed layer depth, wind speed, or day of year), using year as an interacting categorical variable. The latter is because it is possible that a pattern of environmental variable versus rate does not appear within a specific cruise due to spatial variability but is still important for explaining variability on an interannual basis. Adjusted R^2 values (adjusted to take into account the increase in R^2 simply due to the complexity of the model increasing) of significant correlations are listed in Table 2 and complete coefficients for all the multilinear regressions are listed in Table S3. Including time since ice melted as a variable or including salinity as a predictor variable did not strongly influence the goodness of fit nor did using volumetric rates as response variables (Table S3). Plots of NCP and GOP versus selected environmental variables (ice cover, N^2, and phosphate) show that GOP and NCP are significantly ($p < 0.05$) but weakly negatively correlated to ice concentration and are generally positively correlated to N^2 and phosphate (Figure 4), although in some individual years, there are negative correlations with N^2 (e.g., 2011, 2014, and 2015). The ratio NCP:GOP is significantly, but weakly, correlated with ice cover, wind speed, and day of year.

One drawback of using year as a categorical variable, however, is that some of the observed correlations may simply be due to the connection between year and rate, rather than due to the environmental variable. Thus, the adjusted R^2 values were compared to a correlation between GOP (or NCP or NCP/GOP) and year (as categorical variable) and in Table 2, values in bold correspond to multiple linear correlations in which including the environmental variable increases the goodness of fit. This was the case for GOP for ice concentration, PO_4, SiO_4, and mixed layer depth; for NCP for ice concentration, N^2, PO_4, SiO_4, and mixed layer depth; and for NCP/GOP for ice concentration, day of year and wind speed.

Regressions calculated with volumetric GOP and NCP (Tables S4 and S5) show similar values to those calculated with mixed layer integrated GOP and NCP, with the exception of there being a much larger correlation coefficient with mixed layer depth than there is in the case of the aerial rates. Shallower mixed layer depths can lead to the phytoplankton spending more time in a higher light regime, and thus, there is indeed a physical basis for the strong correlation shown. However, the correlation may not be as significant as it appears because the mixed layer depth was used directly to calculate the volumetric rate.

Multilinear regressions were also calculated using NCP as a response variable and GOP as a predictor variable in order to test the hypothesis that the amount of NCP is controlled in large part by the amount of total photosynthesis occurring. Perhaps unsurprisingly, the correlations between NCP with GOP were stronger

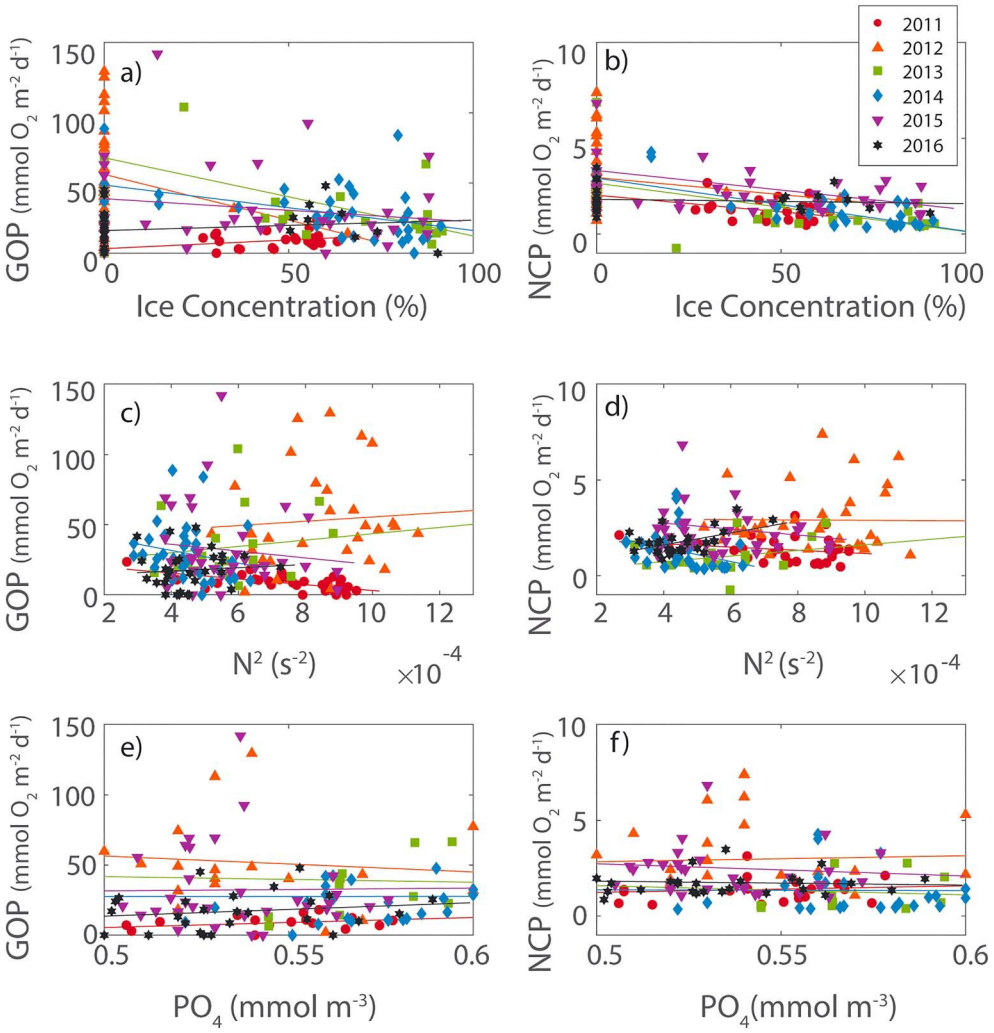

Figure 4. Property-property plots of (a) GOP and ice concentration, (b) NCP and ice concentration, (c) GOP and stratification index N^2, (d) NCP and stratification index N^2, (e) GOP and phosphate, and (f) NCP and phosphate. Colors reflect the different years in which data were collected. Lines are simple linear regressions for data solely within that year.

than between NCP and any of the environmental variables (with year as a categorical variable: adjusted $R^2 = 0.51$, $p < 0.01$; without year as categorical variable: $R^2 = 0.37$, $p < 0.01$). These correlations became even stronger if ice was included as an additional predictor variable (adjusted $R^2 = 0.60$, $p < 0.01$).

Multilinear regressions using two environmental variables to predict rates of NCP or GOP were also calculated and the strongest correlations were found between GOP with ice cover and phosphate as predictor variables (adjusted $R^2 = 0.31$, $p < 0.01$) and between NCP with ice cover and N^2 as predictor variables (adjusted $R^2 = 0.34$, $p < 0.01$). Additionally, simple linear correlations were also calculated between each one of the three response variables (GOP, NCP, and NCP/GOP) and one environmental variable (ice cover, N^2, PO_4, SiO_4, mixed layer depth, day of year, and winds). With the exception of the correlation between NCP and ice cover ($R^2 = 0.22$), all the R^2 values were small but they were significant in several cases (Table S4).

4.2. Principal Component Analysis

In order to further explore the possible causes for the observed variance in NCP and GOP, a principal component analysis was performed. A principal component analysis between NCP, GOP, ice concentration, N^2, phosphate, and silicate reveals that the first three factors explain 80% of the variance. Loadings of each variable on the factors are in Table S6. Factor 1, which explains 41% of the total variance in the data, includes

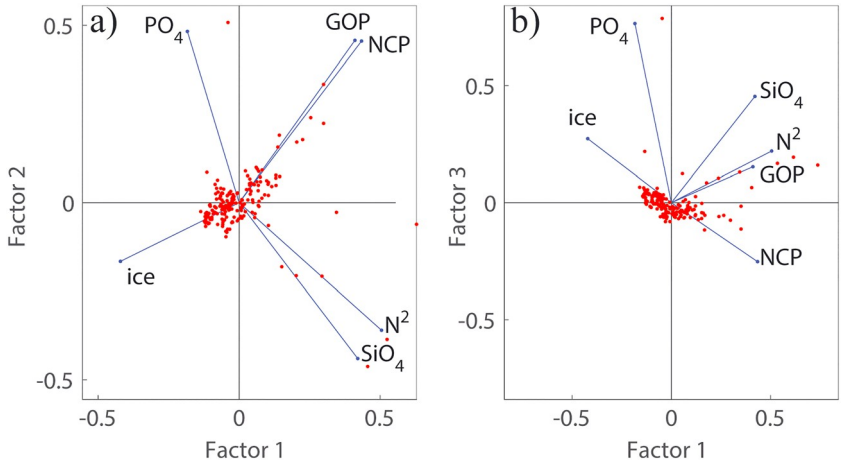

Figure 5. Biplot of (a) factors 1 and 2 and (b) of factors 1 and 3 of the PCA analysis described in the text. NCP and GOP cluster closely in the first plot, signifying their strong relationship with each other. Ice concentration is negatively related to NCP and GOP. In the second biplot, ice and NCP are negatively related and N^2 and GOP cluster together.

negative loadings of ice, and positive loadings of GOP, NCP, N^2, and silicate. Factor 2 which explains 24% of the total variance includes positive loadings of GOP, NCP, and phosphate and negative loadings of N^2, and silicate. Interestingly, N^2 and GOP and NCP show the same sign loading on factor 1, suggesting that an increase in stratification leads to overall higher productivity, but the opposite sign loading on factor 2. Given that the nutrients more strongly load on factor 2, this may be showing that the increase in stratification reduces the amount of nutrients available and thus also has a negative effect on production. A biplot of factors 1 and 2 (Figure 5a) shows that NCP and GOP are closely linked with ice cover being negatively related to them. A biplot of factors 1 and 3 (Figure 5b) suggests that N^2 is closely related to GOP and that NCP and ice extent are inversely related.

4.3. Sea Ice Extent and NCP and GOP

Perhaps the largest change in environmental conditions in the Arctic is the dramatic loss of sea ice with fractional ice coverage now routinely below the previous 30-year average (Stroeve et al., 2012). Several observations from the data presented here support the conclusion that a decrease in sea ice will likely increase GOP and to a lesser extent NCP in this region of the Arctic, at least until nutrients become scarce. First, the most significant correlations found between any environmental variable and NCP or GOP are between sea ice concentration and NCP or between sea ice concentration and GOP. This is true whether the ice concentration from the day of measurement is used or whether a weighted ice concentration (similar weighting scheme as is used in gas exchange) is used. Additionally, this is true if the entire data set is considered, or just the summer cruises or just the fall cruises. The correlation between sea ice and GOP is weaker if just the fall cruises are considered than if just the summer cruises are considered, perhaps because by fall, nutrients are starting to become limiting and thus decreased sea ice, although leading to more light penetration, can only boost productivity so far. The correlation between ice extent and NCP is similar for the summer cruises and fall cruises. However, even though correlation with ice extent is the strongest of any of the environmental correlations, correlation does not imply causation and additionally, the correlation with ice extent, including year as an interactive, categorical variable, still can only explain up to 30% of the variance in GOP and NCP.

The factor loadings in the PCA point also to a negative relationship between GOP and sea ice concentration and between NCP and sea ice concentration. It is interesting that ice had the seemingly largest effect on GOP and NCP of the environmental forcings considered (i.e., nutrients, stratification, winds) even in this region of the Arctic, which is known to be one of the most oligotrophic regions. Some studies have theorized that a lack of sea ice may not lead to higher production because nutrients will become limiting (Carmack & McLaughlin, 2011; Tremblay et al., 2015; Wassmann, 2015). This study was too short to be able to determine if that is the case but at least in the time frame studied, it seems that even though Canada Basin is very low in

nutrients, production is increasing as sea ice extent decreases and that productivity is more sensitive to sea ice extent than to nutrient concentration.

The loss of all sea ice in the sampling grid in 2012 may have been a tipping point for GOP. Notably, mean GOP increased by a factor of 7 during the extremely low sea ice summer of 2012 (compared to summer of 2011). Although GOP slowly decreased in subsequent years, it remained above the 2011 level. What is the reason for this dramatic change? One possibility is that it has to do with the amount of multiyear sea ice. Since nearly all the ice in the sampling grid melted in the summer of 2012 (the sampling was extended northward that year in order to sample at some partially ice-covered stations), the ice in 2013 may have been primarily first year ice, which is known to have different optical properties than multiyear ice (Katlein et al., 2015; Light et al., 2015). However, since much of the sea ice in the Canada Basin is advected from the Canadian Archipelago, the springs and summers of 2013 and 2014 may have actually had larger fractions of multiyear sea ice than 2011 (Howell et al., 2016; Tooth & Tschudi, 2018), suggesting that some other environmental or biological factor must be responsible for the shift in GOP to higher values starting in 2012. It will be intriguing to see whether GOP increases sharply again if/when there is another summer with sea ice as low as 2012.

Unfortunately, we have no data before 2011 and thus we cannot unequivocally prove that the cause for the dramatic increase in GOP between 2011 and 2012 is a result of the loss of sea ice. Indeed, a second reasonable hypothesis is that it is not that 2012 has unusually high GOP that persisted for many years but rather that 2011 has much lower GOP than the other years because the cruise in 2011 was approximately two weeks earlier and was before the summer increase in stratification (see section 4.4 for more details on this argument). Very little in situ data exist for primary productivity rates in the Beaufort Gyre, and thus, we were not able to use other in situ data to determine if the step change observed in our data between 2011 and 2012 is observed elsewhere. Remote sensing algorithms have been applied in the Arctic; Arrigo and Van Dijken (Arrigo & van Dijken, 2015) show only a modest increase in net primary production rates between 2011 and 2012 in the Canada Basin. The remote sensing technique, however, only estimates productivity at the very surface of the ocean, does not work through clouds, and misses under ice blooms, and previous work has shown that the triple oxygen isotope technique and remote sensing algorithm do not agree well in the Canada Basin (Stanley et al., 2015).

Increased GOP corresponding to decreased ice concentration can be explained by a decrease in ice leading to an increase in light penetration and thus an increase in photosynthesis. In the surface ocean, in the summertime when mixed layers are shallow, the mixed layer production is less likely to be light limited than production at deeper depths within the euphotic zone. Nonetheless, light penetration is decreased by sea ice cover (Nicolaus et al., 2012) and thus low light still could be reducing productivity in the partially sea ice-covered regions (during the summer 2013 cruise, sea ice concentrations were as high as 80% at some stations). Additionally, an alternative hypothesis as to why the decreased sea ice concentration could lead to an increase in production is that submesocale dynamics are increased when there is little or no sea ice (Mensa et al., 2018) but depressed under sea ice (Mensa & Timmermans, 2017; Timmermans et al., 2012). Since the region has very low nutrients within the mixed layer, perhaps when sea ice cover is decreased, more nutrients are delivered through submesoscale motions and thus GOP increases.

It is less intuitive to understand why NCP is negatively correlated with sea ice concentration. Part of the reason may be that as GOP increases, heterotrophic and autotrophic respiration also increase to consume the new organic matter fixed in photosynthesis but the increased respiration does not match the increase in GOP, leading to an increase in NCP. Indeed, the largest predictor of NCP was GOP, supporting the above mechanism. Another possibility is that since ice can serve as a habitat for heterotrophs (Boetius et al., 2015), the loss of sea ice results in a smaller heterotrophic population and thus a larger carbon export. Third, submesoscale dynamics have been shown in models (Lévy et al., 2012; Resplandy et al., 2012) and in observations (Estapa et al., 2015; Stanley et al., 2017) to likely lead to increased export and NCP; thus, an increase in submesoscale dynamics resulting from loss of sea ice would likely increase NCP.

Recent work has highlighted the importance of massive blooms of phytoplankton under sea ice (Arrigo et al., 2012; Lowry et al., 2018). No such blooms were observed during the cruises for this study, perhaps because under ice blooms would have occurred earlier in the season than the cruises occurred. Thus, the conclusions

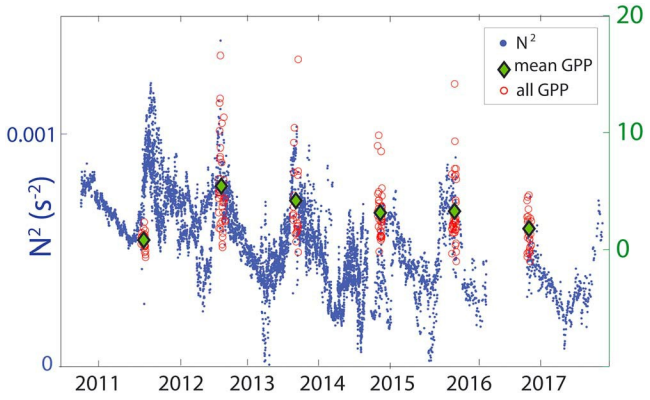

Figure 6. (left axis) N^2, the Brunt Väisälä frequency, a measure of the stratification, as calculated from ice-tethered profiles in the Canada Basin and from the CTD casts during the study period. (right axis) The mean GOP (green) and all the rates of GOP (red) as measured at the stations during the cruises.

in this paper cannot be used to determine an effect that melting sea ice might have on early season primary productivity or to address whether the increase in productivity accompanying a possible decrease in sea ice will compensate for the potential decrease in productivity if such under ice blooms cease.

4.4. Stratification and NCP and GOP

Rates of NCP and GOP were significantly positively correlated with N^2, an index of stratification. An increase in stratification would lead to phytoplankton spending more time in a higher light regime, which could lead to increased photosynthesis if the phytoplankton were light limited. Interestingly, the reverse relationship of NCP and GOP with stratification (i.e., negative correlation) would be expected if the phytoplankton were nutrient limited since increased stratification is usually associated with lower levels of nutrients. Light-limited phytoplankton would be quite sensitive, presumably, to loss of sea ice and thus the relationship between stratification and GOP is consistent with the above observations about the relationship between sea ice and GOP.

NCP is positively correlated with stratification, in part at least, because of the inherent link between GOP and NCP. Thus, as explained above, since GOP increases with stratification, so does NCP. NCP also would increase with increased stratification if the heterotrophic community is more sensitive to the decrease in nutrients caused by increased stratification than the autotrophic community is. This would cause a reduction in community respiration and thus an increase in net community production.

It is possible that stratification earlier in the season is more important for determining rates of GOP and NCP than the stratification at the moment of sample collection. To investigate this, N^2 was calculated from profiles from all ITPs that were in the Beaufort Gyre between 2011 and 2016 (Figure 6). The ITP missions used here ranged from 0.5 to 3 years, and thus, none of the ITPs provided data for the entire period. The data show that the 2011 cruise, which occurred approximately two weeks earlier in the year than the other summer cruises, occurred before the summer increase in stratification, whereas the other cruises took place after the summer increase in stratification had started. Thus, a hypothesis for the much smaller GOP observed in 2011 compared to the other years is that it was a result of the timing of the cruise with respect to onset of stratification. Indeed, there is a strong correlation between seasonal mean GOP and mean N^2, even if the data from 2011 are excluded since the 2011 data is in a different stratification regime ($R^2 = 0.64$, $p = 0.08$, Kendall due to small number of samples when comparing means). More work needs to be done on elucidating the connection between stratification and rates of primary productivity.

4.5. Nutrients and NCP and GOP

Nitrogen is likely the limiting nutrient in the Canada Basin (Ardyna et al., 2017; Codispoti et al., 2013; Varela et al., 2013). However, nitrate levels were undetectable (<0.05 mmol/m^3) in almost all surface samples and thus all analysis presented here is of phosphate and silicate. NCP and GOP were both correlated with phosphate, with phosphate concentrations predicting 23% of the variance in GOP and 18% of the variance in NCP when year was used as an interacting categorical variable. Silicate, a nutrient important for diatoms, explained 24% of the variance in GOP and 22% of the variance in NCP with usually a positive correlation. Notably, within a year, correlations with nutrients were usually not significant and were sometimes negative.

Notched box and whisker plots (Figure S2) and spatial maps (Figure S5) show that phosphate concentrations did not differ significantly between the summer cruises and the fall cruises. In the fall, more nutrients may be accessible because of the deeper mixed layers but also more time has elapsed since the ice has melted and thus more nutrients may have been consumed. These competing effects may lead to similar overall nutrient levels. Phosphate concentrations were significantly higher in 2013 and 2014 than in other years. These were both years with highest ice cover and lowest NCP/GOP. However, the ratio of NCP/GOP is not significantly correlated with phosphate.

Nutrients can be brought to the surface following transient mixing due to high wind events. In particular, during the 2012 cruise, winds were higher than usual (Figures S2 and S6), which may in turn have contributed to the larger than usual GOP and NCP that year. Indeed in 2012, winds are significantly correlated with both GOP and NCP (Table S3). Additionally, observations from ice-tethered profiles, in conjunction with the cruise data, show that near the end of the 2012 cruise (on 5 September), a storm was observed with increased wind speeds, the mixed layer deepened, and some nitrate was detectable within the mixed layer, which could in turn have led to increased production (Islam et al., 2017). Furthermore, also in 2012, a major gale in the Arctic occurred just before sampling on the cruise commenced (Parkinson & Comiso, 2013), and thus, the higher production we observe in 2012 could in part be related to nutrients upwelled during that storm. Over the entire six-year data set, however, winds have a significant but relatively weak correlation with NCP and do not show an overall correlation with GOP (Table 2).

Positive NCP is observed throughout all the cruises even though no nitrate was usually detected in the mixed layer. This situation is similar to the subtropics, where there has been a longstanding conundrum of positive NCP in summer despite no detectable nitrates (e.g., Michaels et al., 1994). One possible explanation, often used for the subtropics, is that submesoscale processes may be locally delivering nutrients (Lévy et al., 2012) that are then consumed by organisms so quickly that nitrate levels are undetectable by regular measurements. A similar process may be happening here—recent work showed prevalent submesoscale dynamics in the early fall in the Beaufort Gyre (Mensa et al., 2018). Additionally, some of the required nitrogen could be supplied by nitrogen fixation, a process that was recently reported to occur in the Arctic Ocean (Harding et al., 2018; Sipler et al., 2017) or by urea (Varela et al., 2013).

4.6. Community Structure

Even if all the environmental variables considered are used together in a multilinear regression (ice cover, N^2, phosphate, silicate, mixed layer depth, day of year, winds), only 38% of variance in GOP and 37% variance in NCP is explained. The PCA shows that more of the variance can be explained by a combination of variables; 40% of the variance in GOP and 46% of the variance in NCP can be explained by the first three factors. That still leaves a lot of variability that cannot be accounted for by the environmental parameters measured. What could be responsible for this variability? Additionally, the factor with the largest loadings of GOP and NCP in the PCA (factor 5) has very small loadings of the environmental variables, also suggesting that an unknown parameter is important for explaining the observed variability in GOP and NCP.

One likely choice for this important unknown is the community structure, that is, exactly which phytoplankton, zooplankton, and bacteria are present each season. It has been shown that community structure is changing in the Canada Basin (Blais et al., 2017; Li et al., 2009). Unfortunately, we do not have community structure data associated with the data presented in this study so we cannot assess how changes in community structure are affecting variability in GOP and NCP and whether those changes could explain the rest of the variability that is observed. However, to get a rough idea, we calculated an algorithmic community composition estimate using the neural-network-based method of Sauzède et al. (2015). Sauzède et al. trained and validated a neural network using 896 vertical profiles of pigments and fluorescence representative of the global ocean (some of which were in the Arctic). We combined their resulting algorithm with in situ fluorescence profiles measured on our cruises in order to estimate concentrations of various size classes. Correlations of GOP and NCP with the algorithm's total chlorophyll, microphytoplankton, nanophytoplankton, and picophytoplankton concentrations were found to be significant ($p < 0.05$) with R^2 ranging from 0.05 to 0.4 (Figure S8). GOP and NCP were most strongly correlated with the algorithm's estimate of microphytoplankton community, which includes diatoms. Diatoms have been shown to be increasing in the Beaufort Sea (corresponding to our stations south of 72°N; Blais et al., 2017) but decreasing in the Beaufort Gyre itself (N of 72°N; Li et al., 2009; Zhuang et al., 2018). Diatoms are expected, in general, to contribute to greater export since their increased size can lead to more efficient sinking out of the upper ocean. If they are also contributing to greater photosynthesis, then GOP and NCP would both be positively correlated with the algorithm's estimate of microphytoplankton concentration (as is seen in Figure S8) but the NCP/GOP ratio would not be. Indeed, we found stronger relationships between NCP and GOP separately with community structure parameters than between their ratio and community structure; correlations between the ratios of NCP/GOP and community components had $R^2 < 0.1$ in all cases.

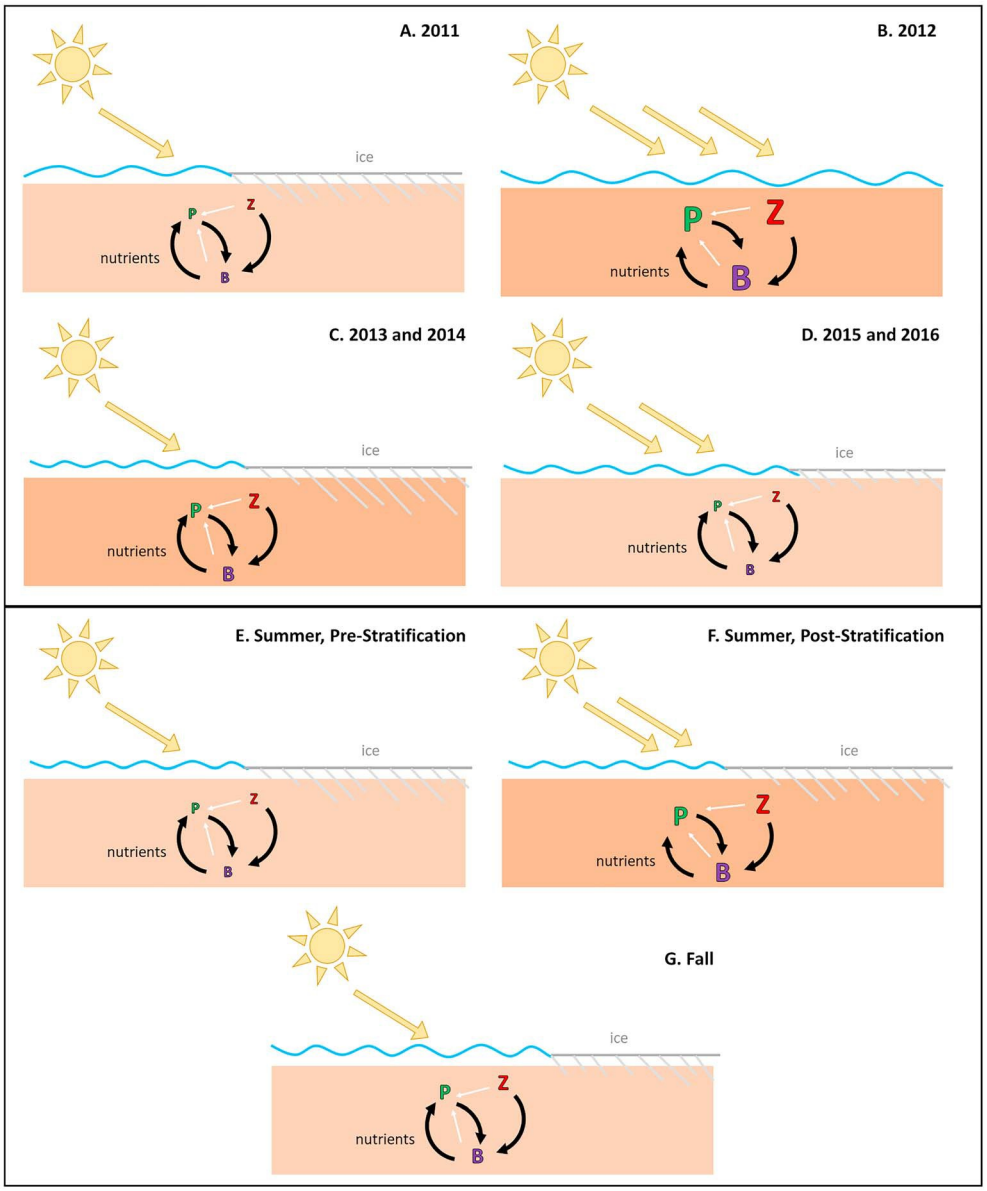

Figure 7. Schematic of two potential models for the state of productivity in the Canada Basin of the Arctic Ocean. Phytoplankton (green P) produces more oxygen in optimal conditions of light penetration and excess nutrients. Grazing pressures (white arrows) from both zooplankton (red Z) and bacteria (purple B) also results in the cycling of nutrients (black arrows) through the microbial loop. In the first model, productivity is affected greatly by sea ice concentration. (a) The "base" state in 2011 shows moderate levels of ice and nutrients. (b) During the extreme sea ice loss in 2012, productivity increases due to greater sunlight penetration. (c) The ice rebounds quickly, leading to smaller productivity than in 2012, although the ice may be younger than before the melting event. (d) Over time, the ice becomes older and also, because the cruises are later in the year, nutrients are more limited and productivity decreases. In the second model, productivity is governed by a seasonal progression. (e) At the start of the summer, before the onset of summer stratification, productivity is low. (f) Then, once stratification greatly increases, productivity increases as well, perhaps because the phytoplankton have more time in increased light. (g) In the fall, production decreases slightly as mixed layers deepen and nutrient levels decrease slightly. Each panel shows a simple schematic of the potential effects of ice concentration (gray), light penetration (yellow arrows), and nutrient availability (intensity of orange indicates nutrient levels) based on the six years of data from this study.

5. Conclusions

Both penetration of light and availability of nutrients likely play a critical role in leading to higher GOP at various locations. If 2011 is considered a reference for phytoplankton productivity before the dramatic loss of sea ice in 2012, multiyear ice, although already depleted compared to historic values (Comiso, 2012), may have been a factor in a decreased light availability for phytoplankton in 2011, resulting in significantly lower GOP (Figure 7 for conceptual schematic). Conversely, the lower GOP in 2011 may be due to the cruise occurring earlier in the year compared to the onset of summer stratification. In any case, in 2012, the introduction of more light penetration through the loss of sea ice and the availability of nutrients likely created optimal conditions for phytoplankton production and subsequently for a stronger proportional respiration from zooplankton and bacteria (Figure 7b). In both 2013 and 2014, the availability of phosphate was relatively high throughout the study area and though sea ice extent on average was high, the most productive regions were those in which sea ice concentration was low (Figure 7c). Interestingly, the data from these years yielded similar results to each other, but were from different seasons. Moving into 2015 and 2016, phosphate concentrations strongly followed the gradient of sea ice extent: relatively lower in open waters and higher in sea ice covered waters. These results imply that the penetration of light is a critical factor during the earlier years of this study when nutrients were possibly available in excess amounts. It is possible that these nutrient levels get depleted and the study area became nutrient limited over time, as suggested by the results in 2015 and 2016. The overall productivity in those two years was lower than in 2012 (Figure 7d), likely because these cruises occurred later in the year when nutrients were depleted and/or because ice concentrations, though lower than in 2011, 2013, or 2014, were higher than in 2012.

An alternative hypothesis describes the observed productivity rates in terms of a seasonal progression. In this conceptual model, 2011 has lowest GOP because the cruise occurred before the summer increase in stratification (Figure 7e). GOP increased and remained high in 2012 and 2013 because both cruises were in the summer (Figure 7f) when mixed layer depths were shallow and light was plentiful. Respiration rates were also high and thus NCP was only slightly higher than earlier in the season in spite of the increase in GOP. In the fall, GOP decreased slightly as light and nutrients became less available (Figure 7g). Respiration slowed as well and thus once again NCP remained similar to the other seasons.

Our data do not definitively suggest which hypothesis is a better representation of productivity dynamics in the Beaufort Gyre. When considering rates integrated over the depth of the mixed layer (the focus of this paper), the similarity in NCP and the NCP/GOP ratio between 2013 and 2014 (different seasons) as well as the fact that the median GOP was similar in 2013–2015 (different seasons) gives slight preference to the connection with sea ice hypothesis (Figures 7a–7d) rather than the seasonal one (Figures 7e–7g). However, volumetric rates in NCP and GOP (Figure S1) show a striking seasonal difference and support the seasonal hypothesis. The differences in NCP and GOP between 2011 and 2012 can be explained equally well by both hypotheses. Furthermore, the hypotheses are not mutually exclusive since both seasonal timing and ice concentrations could be important for setting productivity levels.

In summary, the rates of mixed layer GOP and NCP presented in this study from the summers of 2011–2013 and falls of 2014–2016 have demonstrated that there is large spatial and interannual variability in these key carbon cycle parameters throughout the Canada Basin. In 2012, mean GOP was found to be 7 times greater than that in 2011. Moreover, following 2012, GOP remained higher than in 2011, which suggests that the extreme loss of sea ice extent in 2012 may have had a critical effect on primary productivity. NCP was not found to be significantly different from year to year, which suggests that mixed layer dissolved inorganic carbon drawdown has remained about the same seasonally and interannually. Ultimately, while primary producers in this area are more photosynthetically productive, the community may respond by efficiently respiring the increased available carbon.

Together, these results suggest that if the Arctic sea ice continues to melt, the increase in light exposure may lead to higher productivity by primary producers initially but create a nutrient limited environment over time. These conclusions are consistent with the mixed layer rates calculated from gas tracer data from these six years in the Beaufort Gyre area of the Canada Basin but are not definitive predictions for the future state of the entire Arctic Ocean nor for what is occurring in water below the mixed layer depth.

Acknowledgments

We sincerely thank the scientific teams of Fisheries and Oceans Canada's Joint Ocean Ice Studies expedition and Woods Hole Oceanographic Institution's Beaufort Gyre Observing System. The hydrographic, nutrient, and chlorophyll data were collected and made available by the Beaufort Gyre Exploration Program based at the Woods Hole Oceanographic Institution (http://www.whoi.edu/beaufortgyre) in collaboration with researchers from Fisheries and Oceans Canada at the Institute of Ocean Sciences. We thank the captains and crews of the Canadian icebreaker CCGS Louis S. St-Laurent and Mike Dempsey for sample collection. This paper was improved by the suggestions of Michael DeGrandpre and one anonymous reviewer. We are grateful to Qing Wang at Wellesley College for her assistance with statistics. We thank our funding sources: the National Science Foundation (NSF 1547011, NSF 1302884, NSF 1719280, NSF 1643735) and the support of Fisheries and Oceans Canada. Data presented and discussed in this paper can be found in the Arctic Data Center (http://10.18739/A2W389).

References

Abbott, B. W., Jones, J. B., Schuur, E. A. G., Chapin, F. S., Bowden, W. B., Bret-Harte, M. S., et al. (2016). Biomass offsets little or none of permafrost carbon release from soils, streams, and wildfire: an expert assessment. Environmental Research Letters, 11(3). https://doi.org/10.1088/1748-9326/11/3/034014

Ardyna, M., Babin, M., Devred, E., Forest, A., Gosselin, M., Raimbault, P., & Tremblay, J. E. (2017). Shelf-basin gradients shape ecological phytoplankton niches and community composition in the coastal Arctic Ocean (Beaufort Sea). Limnology and Oceanography, 62(5), 2113–2132. https://doi.org/10.1002/lno.10554

Ardyna, M., Babin, M., Gosselin, M., Devred, E., Belanger, S., Matsuoka, A., & Tremblay, J. E. (2013). Parameterization of vertical chlorophyll a in the Arctic Ocean: Impact of the subsurface chlorophyll maximum on regional, seasonal, and annual primary production estimates. Biogeosciences, 10(6), 4383–4404. https://doi.org/10.5194/bg-10-4383-2013

Ardyna, M., Babin, M., Gosselin, M., Devred, E., Rainville, L., & Tremblay, J. E. (2014). Recent Arctic Ocean sea ice loss triggers novel fall phytoplankton blooms. Geophysical Research Letters, 41, 6207–6212. https://doi.org/10.1002/2014GL061047

Arrigo, K. R., Perovich, D. K., Pickart, R. S., Brown, Z. W., van Dijken, G. L., Lowry, K. E., et al. (2012). Massive phytoplankton blooms under Arctic sea ice. Science, 336(6087), 1408. https://doi.org/10.1126/science.1215065

Arrigo, K. R., & van Dijken, G. L. (2015). Continued increases in Arctic Ocean primary production. Progress in Oceanography, 136, 60–70. https://doi.org/10.1016/j.pocean.2015.05.002

Barkan, E., & Luz, B. (2003). High-precision measurements of O-17/O-16 and O-18/O-16 of O-2 and O-2/Ar ratio in air. Rapid Communications in Mass Spectrometry, 17(24), 2809–2814. https://doi.org/10.1002/rcm.1267

Barwell-Clarke, J., & Whitney, F. (1996). Institute of Ocean Sciences Nutrient Methods and Analysis. Can. Tech. Rep. Hydrogr. Ocean Sci. 182: vi + 43 p. Sidney, B.C.

Bates, N. R., Cai, W. J., & Mathis, J. T. (2011). The ocean carbon cycle in the western Arctic Ocean distributions and air-sea fluxes of carbon dioxide. Oceanography, 24(3), 186–201. https://doi.org/10.5670/oceanog.2011.71

Blais, M., Ardyna, M., Gosselin, M., Dumont, D., Belanger, S., Tremblay, J. E., et al. (2017). Contrasting interannual changes in phytoplankton productivity and community structure in the coastal Canadian Arctic Ocean. Limnology and Oceanography, 62(6), 2480–2497. https://doi.org/10.1002/lno.10581

Boetius, A., Anesio, A. M., Deming, J. W., Mikucki, J. A., & Rapp, J. Z. (2015). Microbial ecology of the cryosphere: Sea ice and glacial habitats. Nature Reviews. Microbiology, 13(11), 677–690. https://doi.org/10.1038/nrmicro3522

Boisvert, L. N., & Stroeve, J. C. (2015). The Arctic is becoming warmer and wetter as revealed by the Atmospheric Infrared Sounder. Geophysical Research Letters, 42, 4439–4446. https://doi.org/10.1002/2015GL063775

Butterworth, B. J., & Miller, S. D. (2016). Air-sea exchange of carbon dioxide in the Southern Ocean and Antarctic marginal ice zone. Geophysical Research Letters, 43, 7223–7230. https://doi.org/10.1002/2016GL069581

Cai, W. J., Chen, L. Q., Chen, B. S., Gao, Z. Y., Lee, S. H., Chen, J. F., et al. (2010). Decrease in the CO_2 uptake capacity in an ice-free Arctic Ocean basin. Science, 329(5991), 556–559. https://doi.org/10.1126/science.1189338

Carmack, E., & McLaughlin, F. (2011). Towards recognition of physical and geochemical change in Subarctic and Arctic Seas. Progress in Oceanography, 90(1-4), 90–104. https://doi.org/10.1016/j.pocean.2011.02.007

Carmack, E. C., Yamamoto-Kawai, M., Haine, T. W. N., Bacon, S., Bluhm, B. A., Lique, C., et al. (2016). Freshwater and its role in the Arctic Marine System: Sources, disposition, storage, export, and physical and biogeochemical consequences in the Arctic and global oceans. Journal of Geophysical Research: Biogeosciences, 121, 675–717. https://doi.org/10.1002/2015JG003140

Castro-Morales, K., & Kaiser, J. (2012). Using dissolved oxygen concentrations to determine mixed layer depths in the Bellingshausen Sea. Ocean Science, 8(1), 1–10. https://doi.org/10.5194/os-8-1-2012

Cavalieri, D. J., C. L. Parkinson, P. Gloersen, and H. J. Zwally (1996), Sea ice concentrations from Nimbus-7 SMMR and DMSP SSM/I-SSMIS Passive Microwave Data, version 1. Daily Northern Subset, edited by N. N. S. A. I. D. C. D. A. A. Center, Boulder, Colorado USA.

Codispoti, L. A., Kelly, V., Thessen, A., Matrai, P., Suttles, S., Hill, V., et al. (2013). Synthesis of primary production in the Arctic Ocean: III. Nitrate and phosphate based estimates of net community production. Progress in Oceanography, 110, 126–150. https://doi.org/10.1016/j.pocean.2012.11.006

Comiso, J. C. (2012). Large decadal decline of the Arctic multiyear ice cover. Journal of Climate, 25(4), 1176–1193. https://doi.org/10.1175/JCLI-D-11-00113.1

Emerson, S., Stump, C., Wilbur, D., & Quay, P. (1999). Accurate measurement of O-2, N-2, and Ar gases in water and the solubility of N-2. Marine Chemistry, 64(4), 337–347. https://doi.org/10.1016/S0304-4203(98)00090-5

Estapa, M. L., Siegel, D. A., Buesseler, K. O., Stanley, R. H. R., Lomas, M. W., & Nelson, N. B. (2015). Decoupling of net community and export production on submesoscales in the Sargasso Sea. Global Biogeochemical Cycles, 29, 1266–1282. https://doi.org/10.1002/2014GB004913

Fanning, K. A., & Torres, L. M. (1991). Rn-222 and Ra-226—Indicators of sea-ice effects on air-sea gas-exchange. Polar Research, 10(1), 51–58. https://doi.org/10.1111/j.1751-8369.1991.tb00634.x

Goldman, J. A. L., Kranz, S. A., Young, J. N., Tortell, P. D., Stanley, R. H. R., Bender, M. L., & Morel, F. M. M. (2015). Gross and net production during the spring bloom along the Western Antarctic Peninsula. The New Phytologist, 205(1), 182–191. https://doi.org/10.1111/nph.13125

Greene, C. (2016), Arctic Sea Ice, in MATLAB File Exchange, edited, p. Easily download and plot daily Arctic sea ice concentration grids.

Harding, K., Turk-Kubo, K. A., Sipler, R. E., Mills, M. M., Bronk, D. A., & Zehr, J. P. (2018). Symbiotic unicellular cyanobacteria fix nitrogen in the Arctic Ocean. Proceedings of the National Academy of Sciences of the United States of America, 115(52), 13,371–13,375. https://doi.org/10.1073/pnas.1813658115

Hendricks, M. B., Bender, M. L., & Barnett, B. A. (2004). Net and gross O-2 production in the Southern Ocean from measurements of biological O-2 saturation and its triple isotope composition. Deep-Sea Research Part I: Oceanographic Research Papers, 51(11), 1541–1561. https://doi.org/10.1016/j.dsr.2004.06.006

Ho, D. T., Wanninkhof, R., Schlosser, P., Ullman, D. S., Hebert, D., & Sullivan, K. F. (2011). Toward a universal relationship between wind speed and gas exchange: Gas transfer velocities measured with (3)He/SF(6) during the Southern Ocean Gas Exchange Experiment. Journal of Geophysical Research, Oceans, 116(7), 116, C00F04. https://doi.org/10.1029/2010JC006854

Howell, S. E. L., Brady, M., Derksen, C., & Kelly, R. E. J. (2016). Recent changes in sea ice area flux through the Beaufort Sea during the summer. Journal of Geophysical Research: Oceans, 121, 2659–2672. https://doi.org/10.1002/2015JC011464

Islam, F., DeGrandpre, M., Beatty, C., Krishfield, R., & Toole, J. (Eds) (2016). Gas exchange of CO_2 and O_2 in partially ice-covered regions of the Arctic Ocean investigated using in situ sensors. IOP Publishing Ltd.

Islam, F., DeGrandpre, M. D., Beatty, C. M., Timmermans, M. L., Krishfield, R. A., Toole, J. M., & Laney, S. R. (2017). Sea surface pCO(2) and O-2 dynamics in the partially ice-covered Arctic Ocean. Journal of Geophysical Research: Oceans, 122, 1425−1438. https://doi.org/10.1002/2016JC012162

Jahn, A., Kay, J. E., Holland, M. M., & Hall, D. M. (2016). How predictable is the timing of a summer ice-free Arctic? Geophysical Research Letters, 43, 9113−9120. https://doi.org/10.1002/2016GL070067

Ji, R. B., Jin, M. B., & Varpe, O. (2013). Sea ice phenology and timing of primary production pulses in the Arctic Ocean. Global Change Biology, 19(3), 734−741. https://doi.org/10.1111/gcb.12074

Juranek, L. W., & Quay, P. D. (2005). In vitro and in situ gross primary and net community production in the North Pacific Subtropical Gyre using labeled and natural abundance isotopes of dissolved O-2. Global Biogeochemical Cycles, 19, GB3009. https://doi.org/10.1029/2004GB002384

Juranek, L. W., & Quay, P. D. (2013). Using triple isotopes of dissolved oxygen to evaluate global marine productivity. In C. A. Carlson & S. J. Giovannoni (Eds.), Annual Review of Marine Science (Vol. 5, pp. 503−524). Palo Alto: Annual Reviews.

Katlein, C., Arndt, S., Nicolaus, M., Perovich, D. K., Jakuba, M. V., Suman, S., et al. (2015). Influence of ice thickness and surface properties on light transmission through Arctic sea ice. Journal of Geophysical Research: Oceans, 120, 5932−5944. https://doi.org/10.1002/2015JC010914

Krishfield, R., Toole, J., Proshutinsky, A., & Timmermans, M. L. (2008). Automated ice-tethered profilers for seawater observations under pack ice in all seasons. Journal of Atmospheric and Oceanic Technology, 25(11), 2091−2105. https://doi.org/10.1175/2008JTECHO587.1

Lévy, M., Iovino, D., Resplandy, L., Klein, P., Madec, G., Treguier, A. M., et al. (2012). Large-scale impacts of submesoscale dynamics on phytoplankton: Local and remote effects. Ocean Modelling, 43-44, 77−93. https://doi.org/10.1016/j.ocemod.2011.12.003

Li, W. K. W., McLaughlin, F. A., Lovejoy, C., & Carmack, E. C. (2009). Smallest algae thrive as the Arctic ocean freshens. Science, 326(5952), 539−539. https://doi.org/10.1126/science.1179798

Light, B., Perovich, D. K., Webster, M. A., Polashenski, C., & Dadic, R. (2015). Optical properties of melting first-year Arctic sea ice. Journal of Geophysical Research: Oceans, 120, 7657−7675. https://doi.org/10.1002/2015JC011163

Loose, B., Kelly, R. P., Bigdeli, A., Williams, W., Krishfield, R., van der Loeff, M. R., & Moran, S. B. (2017). How well does wind speed predict air-sea gas transfer in the sea ice zone? A synthesis of radon deficit profiles in the upper water column of the Arctic Ocean. Journal of Geophysical Research: Oceans, 122, 3696−3714. https://doi.org/10.1002/2016JC012460

Loose, B., McGillis, W. R., Perovich, D., Zappa, C. J., & Schlosser, P. (2014). A parameter model of gas exchange for the seasonal sea ice zone. Ocean Science, 10(1), 17−28. https://doi.org/10.5194/os-10-17-2014

Lovely, A., Loose, B., Schlosser, P., McGillis, W., Zappa, C., Perovich, D., et al. (2015). The Gas Transfer through Polar Sea ice experiment: Insights into the rates and pathways that determine geochemical fluxes. Journal of Geophysical Research: Oceans, 120, 8177−8194. https://doi.org/10.1002/2014JC010607

Lowry, K. E., Pickart, R. S., Selz, V., Mills, M. M., Pacini, A., Lewis, K. M., et al. (2018). Under-ice phytoplankton blooms inhibited by spring convective mixing in refreezing leads. Journal of Geophysical Research: Oceans, 123(1), 90−109. https://doi.org/10.1002/2016JC012575

Luz, B., & Barkan, E. (2009). Net and gross oxygen production from O-2/Ar, O-17/O-16 and O-18/O-16 ratios. Aquatic Microbial Ecology, 56(2-3), 133−145. https://doi.org/10.3354/ame01296

Luz, B., & Barkan, E. (2010). Variations of 17O/16O and 18O/16O in meteoric waters. Geochimica et Cosmochimica Acta, 74(22), 6276−6286. https://doi.org/10.1016/j.gca.2010.08.016

Manning, C. C., Howard, E. M., Nicholson, D. P., Ji, B. Y., Sandwith, Z. O., & Stanley, R. H. R. (2017). Revising estimates of aquatic gross oxygen production by the triple oxygen isotope method to incorporate the local isotopic composition of water. Geophysical Research Letters, 44, 10,511−10,519. https://doi.org/10.1002/2017GL074375

McLaughlin, F. A., & Carmack, E. C. (2010). Deepening of the nutricline and chlorophyll maximum in the Canada Basin interior, 2003−2009. Geophysical Research Letters, 37, L24602. https://doi.org/10.1029/2010GL045459

Mensa, J. A., & Timmermans, M. L. (2017). Characterizing the seasonal cycle of upper-ocean flows under multi-year sea ice. Ocean Modelling, 113, 115−130. https://doi.org/10.1016/j.ocemod.2017.03.009

Mensa, J. A., Timmermans, M. L., Kozlov, I. E., Williams, W. J., & Ozgokmen, T. M. (2018). Surface drifter observations from the Arctic Ocean's Beaufort Sea: Evidence for submesoscale dynamics. Journal of Geophysical Research: Oceans, 123(4), 2635−2645. https://doi.org/10.1002/2017JC013728

Michaels, A. F., Bates, N. R., Buesseler, K. O., Carlson, C. A., & Knap, A. H. (1994). Carbon system imbalances in the Sargasso Sea. Nature, 372(6506), 537−540. https://doi.org/10.1038/372537a0

Nicholson, D. P., Stanley, R. H. R., & Doney, S. C. (2014). The triple oxygen isotope tracer of primary productivity in a dynamic ocean. Global Biogeochemical Cycles, 28, 538−552. https://doi.org/10.1002/2013GB004704

Nicolaus, M., Katlein, C., Maslanik, J., & Hendricks, S. (2012). Changes in Arctic sea ice result in increasing light transmittance and absorption. Geophysical Research Letters, 39, L24501. https://doi.org/10.1029/2012GL053738

Nummelin, A., Ilicak, M., Li, C., & Smedsrud, L. H. (2016). Consequences of future increased Arctic runoff on Arctic Ocean stratification, circulation, and sea ice cover. Journal of Geophysical Research: Oceans, 121, 617−637. https://doi.org/10.1002/2015JC011156

Parkinson, C. L., & Comiso, J. C. (2013). On the 2012 record low Arctic sea ice cover: Combined impact of preconditioning and an August storm. Geophysical Research Letters, 40, 1356−1361. https://doi.org/10.1002/grl.50349

Petty, A. A., Stroeve, J. C., Holland, P. R., Boisvert, L. N., Bliss, A. C., Kimura, N., & Meier, W. N. (2018). The Arctic sea ice cover of 2016: A year of record-low highs and higher-than-expected lows. The Cryosphere, 12(2), 433−452. https://doi.org/10.5194/tc-12-433-2018

Prokopenko, M. G., Pauluis, O. M., Granger, J., & Yeung, L. Y. (2011). Exact evaluation of gross photosynthetic production from the oxygen triple-isotope composition of O(2): Implications for the net-to-gross primary production ratios. Geophysical Research Letters, 38, L14603. https://doi.org/10.1029/2011GL047652

Prytherch, J., Brooks, I. M., Crill, P. M., Thornton, B. F., Salisbury, D. J., Tjernstrom, M., et al. (2017). Direct determination of the air-sea CO_2 gas transfer velocity in Arctic sea ice regions. Geophysical Research Letters, 44, 3770−3778. https://doi.org/10.1002/2017GL073593

Resplandy, L., Martin, A. P., Le Moigne, F., Martin, P., Aquilina, A., Memery, L., et al. (2012). How does dynamical spatial variability impact ^{234}Th-derived estimates of organic export? Deep Sea Research, Part I, 68, 24−45. https://doi.org/10.1016/j.dsr.2012.05.015

Reuer, M. K., Barnett, B. A., Bender, M. L., Falkowski, P. G., & Hendricks, M. B. (2007). New estimates of Southern Ocean biological production rates from O-2/Ar ratios and the triple isotope composition of O-2. Deep-Sea Research Part I: Oceanographic Research Papers, 54(6), 951−974. https://doi.org/10.1016/j.dsr.2007.02.007

Sauzède, R., Claustre, H., Jamet, C., Uitz, J., Ras, J., Mignot, A., & D'Ortenzio, F. (2015). Retrieving the vertical distribution of chlorophyll a concentration and phytoplankton community composition from in situ fluorescence profiles: A method based on a neural network with potential for global-scale applications. Journal of Geophysical Research: Oceans, 120, 451−470. https://doi.org/10.1002/2014JC010355

Sipler, R. E., Gong, D. L., Baer, S. E., Sanderson, M. P., Roberts, Q. N., Mulholland, M. R., & Bronk, D. A. (2017). Preliminary estimates of the contribution of Arctic nitrogen fixation to the global nitrogen budget. Limnology and Oceanography Letters, 2(5), 159–166. https://doi.org/10.1002/lol2.10046

Slagstad, D., Wassmann, P. F. J., & Ellingsen, I. (2015). Physical constrains and productivity in the future Arctic Ocean. Frontiers in Marine Science, 2, 85. https://doi.org/10.3389/fmars.2015.00085

Stanley, R. H. R., Jenkins, W. J., Doney, S. C., & Lott, D. E. III (2009). Noble gas constraints on air-sea gas exchange and bubble fluxes. Journal of Geophysical Research, Oceans, 114(C11). https://doi.org/10.1029/2009JC005396

Stanley, R. H. R., McGillicuddy, D. J., Sandwith, Z. O., & Pleskow, H. M. (2017). Submesoscale hotspots of productivity and respiration: Insights from highresolution oxygen and fluorescence sections. Deep Sea Resarch Part I, 130(1–11). https://doi.org/10.1016/j.dsr.2017.10.005

Stanley, R. H. R., Sandwith, Z. O., & Williams, W. J. (2015). Rates of summertime biological productivity in the Beaufort Gyre: A comparison between the low and record-low ice conditions of August 2011 and 2012. Journal of Marine Systems, 147, 29–44. https://doi.org/10.1016/j.jmarsys.2014.04.006

Stroeve, J. C., Serreze, M. C., Holland, M. M., Kay, J. E., Malanik, J., & Barrett, A. P. (2012). The Arctic's rapidly shrinking sea ice cover: A research synthesis. Climatic Change, 110(3-4), 1005–1027. https://doi.org/10.1007/s10584-011-0101-1

Teeter, L., Hamme, R. C., Ianson, D., & Bianucci, L. (2018). Accurate estimation of net community production from O_2/Ar measurements. Global Biogeochemical Cycles, 32. https://doi.org/10.1029/2017GB005874

Timmermans, M. L., Cole, S., & Toole, J. (2012). Horizontal density structure and restratification of the Arctic ocean surface layer. Journal of Physical Oceanography, 42(4), 659–668. https://doi.org/10.1175/JPO-D-11-0125.1

Toole, J. M., Krishfield, R. A., Timmermans, M. L., & Proshutinsky, A. (2011). The ice-tethered profiler: Argo of the Arctic. Oceanography, 24(3), 126–135. https://doi.org/10.5670/oceanog.2011.64

Tooth, M., & Tschudi, M. (2018). Investigating Arctic sea ice survivability in the Beaufort Sea. Remote Sensing, 10(2). https://doi.org/10.3390/rs10020267

Tremblay, J. E., Anderson, L. G., Matrai, P., Coupel, P., Belanger, S., Michel, C., & Reigstad, M. (2015). Global and regional drivers of nutrient supply, primary production and CO_2 drawdown in the changing Arctic Ocean. Progress in Oceanography, 139, 171–196. https://doi.org/10.1016/j.pocean.2015.08.009

Varela, D. E., Crawford, D. W., Wrohan, I. A., Wyatt, S. N., & Carmack, E. C. (2013). Pelagic primary productivity and upper ocean nutrient dynamics across Subarctic and Arctic Seas. Journal of Geophysical Research: Oceans, 118, 7132–7152. https://doi.org/10.1002/2013JC009211

Wanninkhof, R. (2014). Relationship between wind speed and gas exchange over the ocean revisited. Limnology and Oceanography: Methods, 12(6), 351–362. https://doi.org/10.4319/lom.2014.12.351

Wassmann, P. (2015). Overarching perspectives of contemporary and future ecosystems in the Arctic Ocean Preface. Progress in Oceanography, 139, 1–12. https://doi.org/10.1016/j.pocean.2015.08.004

Zhuang, Y. P., Jin, H. Y., Chen, J. F., Li, H. L., Ji, Z. Q., Bai, Y. C., & Zhang, T. Z. (2018). Nutrient and phytoplankton dynamics driven by the Beaufort Gyre in the western Arctic Ocean during the period 2008–2014. Deep-Sea Research Part I: Oceanographic Research Papers, 137, 30–37. https://doi.org/10.1016/j.dsr.2018.05.002